Contribution of nonradiative electron energy losses to the structure of inverse-photoemission spectra

Keith W. Goodman and Victor E. Henrich
Surface Science Laboratory, Department of Applied Physics, Yale University, New Haven, Connecticut 06520
(Received 4 November 1993)

We have considered the effects of electron energy losses on experimentally measured inverse-photoemission spectra. The approximations needed to cast the equations for inverse photoemission into a form such that the measured inverse-photoemission spectrum can be expressed as the convolution of two functions—the true spectrum and a response function—are discussed qualitatively. The true spectrum is the inverse-photoemission spectrum that would result if there were no inelastic background present. The response function is the energy spectrum of the inelastically scattered incident electrons inside the sample; it is modeled by an electron-energy-loss spectrum. The true spectrum is found by deconvoluting the response function from the measured spectrum. This is the first time, to our knowledge, that an experimentally measured response function has been used for background subtraction in ultraviolet inverse photoemission. Results of this background subtraction method are presented for inverse-photoemission spectra of polycrystalline silver and UHV-cleaved $V_2O_5(001)$.

I. INTRODUCTION

Inverse-photoemission spectroscopy (IPES) is used to characterize the unoccupied electronic states of crystalline and polycrystalline solids.[1-3] A well-collimated, monoenergetic electron beam enters a crystal, and the light subsequently emitted from the sample as the incident electrons fall to lower-energy unoccupied states is analyzed in order to deduce the properties of the unoccupied electronic states of the crystal. To this end, conservation laws—one for each one-electron quantum number, i.e., energy, crystal momentum, spin, and the angular symmetry of the electron wave function—are typically used. For example, energy conservation in the spontaneous emission of a photon of energy $\hbar\omega_0$ by an incident electron of energy E_{incident} means that there is an allowed unoccupied electron state at an energy $E_{\text{incident}}-\hbar\omega_0$. However, some of the incident electrons may lose energy prior to photon emission, in which case the initial-state energy of the radiative transition is no longer the incident-electron-beam energy. The higher the incident-electron energy, the greater the number of states into which an incident electron may scatter inelastically before emitting a photon, resulting in the inelastic background characteristic of all IPES spectra.

The IPES spectrum of polycrystalline silver shown in Fig. 1 is characteristic of most IPES spectra: the spectral features are superimposed on a smoothly rising background. One can determine the energy and width of the spectral features directly from the measured spectrum, or a background can first be subtracted from the spectrum; both approaches have been used in the literature, with the majority of studies choosing to analyze IPES spectra with the background present. That approach is adequate for the energy assignment of sharp features at low electron energies where the background is typically small, but at higher electron energies, where the background is correspondingly higher, some assumptions about the background underneath the spectral features must be made in order to obtain accurate values for their energy locations and widths. Even the use of a simple approximation to the actual background, such as a smooth background sketched by hand,[4,5] an integral background,[6,7] or a parabolic background,[8,9] gives some insight into the direction and magnitude that the spectral features in the measured spectrum would shift if the background were not present.

The willingness of authors to use these simple backgrounds is based on an accepted belief that the actual background is indeed a featureless, smoothly rising function of energy.[4,6] Intuitive arguments for the use of a smoothly rising background are straightforward, making it tempting to sketch a background such as the dashed line in Fig. 1, which supposes that the actual spectrum consists of three or four features with little spectral intensity between the features. However, in the approximation that IPES measures the total density of states (DOS)

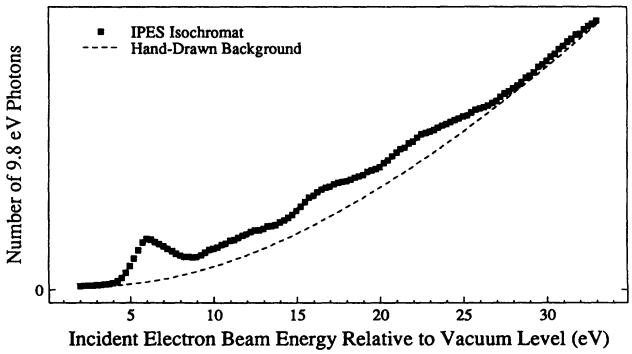

FIG. 1. IPES isochromat spectrum ($\hbar\omega_0=9.8$ eV) of polycrystalline Ag (solid squares) and a hand-drawn background (dashed line).

of polycrystalline samples[10] (or even if this approximation is relaxed somewhat), the true spectral intensity should not go to zero away from the obvious features in the measured spectrum at higher electron energies since the DOS is generally nonzero, and often larger, at higher electron energies. Therefore the hand-drawn background in Fig. 1 is not a reasonable approximation to the actual background.

All of the methods used in the literature to remove the background in IPES and x-ray bremsstrahlung isochromat (BIS) spectra (except hand-drawn[4,5] and parabolic[8,9] backgrounds) are based upon the same model, requiring as input the spectrum of inelastically scattered electrons produced by the incident monoenergetic electron beam. The techniques differ in the methods used to estimate this inelastic spectrum. In this paper we remove the inelastic background from IPES spectra using electron-energy-loss spectroscopy (EELS) to obtain information about the effects of inelastic scattering. None of the previously published background subtraction methods used in ultraviolet IPES use an experimentally determined inelastic spectrum.

In Sec. II our experimental IPES methods are discussed. Section III presents the background subtraction methods that have been used in the literature. Section IV discusses the qualitative differences between backgrounds in angle-integrated and angle-resolved (or "k resolved") IPES (KRIPES) spectra. Section V presents the results of inelastic-background subtraction for the angle-integrated IPES spectrum of polycrystalline Ag and the KRIPES spectrum of UHV cleaved single-crystal $V_2O_5(001)$.

II. EXPERIMENTAL METHODS

The IPES spectra presented in this paper are isochromat (fixed photon energy) spectra. An electron gun[11] produces a collimated beam of monoenergetic electrons that strikes the surface of the sample. Electrons enter the sample by coupling to the unoccupied electronic states of the crystal at the incident-electron energy. Subsequently some of these electrons drop to lower-energy unoccupied states above the Fermi energy E_F via the spontaneous emission of a photon. An isochromat spectrum is generated by sweeping the incident-electron beam energy E_{incident} (the abscissa in Fig. 1), and using a narrow-band photon detector[12] to count the number of $\hbar\omega_0 = 9.8 \pm 0.5$ eV photons that are emitted at each incident energy (the ordinate in Fig. 1).

The polycrystalline Ag sample was cleaned by Ar^+-ion bombardment until no impurities were detected with Auger-electron spectroscopy (AES). Single crystals of $V_2O_5(001)$ were cleaved *in situ* at less than 2×10^{-10} Torr. Ultraviolet photoemission (UPS) spectra of the cleaved surface were characteristic of well-ordered, low-defect-density surfaces. EELS spectra were measured with a double-pass cylindrical mirror analyzer (CMA) equipped with a coaxial electron gun.[13] The energy resolution of the polycrystalline Ag and UHV cleaved $V_2O_5(001)$ EELS spectra was 0.8 and 0.4 eV, respectively.

III. BACKGROUND CORRECTION METHODS

The radiative transition measured in an IPES isochromat spectrum is one from an initial state with energy E_{initial} to a final state with energy E_{final}, where $E_{\text{initial}} - \hbar\omega_0 = E_{\text{final}}$. Typically one assumes that E_{initial} is equal to E_{incident}, so that $E_{\text{incident}} - \hbar\omega_0 = E_{\text{final}}$. Using the latter conservation equation to analyze an IPES spectrum assumes that the initial-state energy of the optical transition is always the incident-beam energy. However, many of the incident electrons suffer inelastic losses prior to the measured radiative transition; thus an IPES spectrum is not generated by a purely monoenergetic source of electrons inside the sample, but rather from an electron source that is distributed in energy.[14] The signal due to the electrons that suffer inelastic losses prior to the radiative transition comprises the inelastic background in the measured spectrum. The total number of $\hbar\omega_0$ photons emitted by a sample bombarded with an electron beam of energy E_{incident}, $I_{\text{measured}}(E_{\text{incident}})$, which includes the inelastic background, is given by

$$I_{\text{measured}}(E_{\text{incident}}) = \int_{E_F+\hbar\omega_0}^{E_{\text{incident}}} R(E_{\text{incident}},E) I_{\text{true}}(E) dE \ , \tag{1}$$

where $R(E_{\text{incident}},E)$ is the energy distribution of electrons inside the sample when a monoenergetic beam of energy E_{incident} strikes the surface of the sample, and $I_{\text{true}}(E)$ is the intensity of the IPES spectrum at E if there were no background present. $I_{\text{true}}(E)$ is found by deconvolving an estimation of the electron source distribution, $R(E_{\text{incident}},E)$, from the measured IPES spectrum, $I_{\text{measured}}(E_{\text{incident}})$. The only technique that has been used in the literature to remove the inelastic background in angle-integrated IPES (Refs. 2, 6, 7, 14, and 15) (except hand-drawn[4,5] and parabolic[8,9] backgrounds) and the two techniques used in x-ray BIS (Refs. 16 and 17) are all based upon Eq. (1), but use different methods to estimate $R(E_{\text{incident}},E)$.

A. Published techniques

Dose and co-workers[2,14,15] calculate $R(E_{\text{incident}},E)$ in several polycrystalline metals, making approximations such that the only input needed for the calculation is the density of both occupied and unoccupied states. Consider first the probability that an incident electron with energy and momentum $E_{\text{incident}}(\mathbf{k}_i)$ scatters to a state $E_{\text{scattered}}(\mathbf{k}_s)$ by the creation of one electron-hole pair with electron energy $E_e(\mathbf{k}_e)$ and hole energy $E_h(\mathbf{k}_h)$. Any electron-hole pair that satisfies the energy and momentum conservation

$$\begin{aligned} &E_{\text{incident}}(\mathbf{k}_i) + E_h(\mathbf{k}_h) = E_{\text{scattered}}(\mathbf{k}_s) + E_e(\mathbf{k}_e) \ , \\ &\mathbf{k}_i + \mathbf{k}_h = \mathbf{k}_s + \mathbf{k}_e + \mathbf{G} \ , \end{aligned} \tag{2}$$

where $\mathbf{G}$ is a reciprocal-lattice vector, will result in the inelastic-energy loss $E_{\text{incident}}(\mathbf{k}_i) \rightarrow E_{\text{scattered}}(\mathbf{k}_s)$. Therefore the probability of a given inelastic loss $P[E_{\text{incident}}(\mathbf{k}_i), E_{\text{scattered}}(\mathbf{k}_s)]$ is the sum of the probabilities for the creation of every electron-hole pair that

satisfies the above constraints. Kane[18] calculates $P[E_{\text{incident}}(\mathbf{k}_i), E_{\text{scattered}}(\mathbf{k}_s)]$ by ignoring momentum conservation, as suggested by Berglund and Spicer,[19] such that the probability for the creation of any particular electron-hole pair is proportional to the normalized product of the electron DOS at E_e and E_h. Relaxing momentum conservation greatly simplifies the calculation of $P[E_{\text{incident}}(\mathbf{k}_i), E_{\text{scattered}}(\mathbf{k}_s)]$. Indeed, the only input needed for the calculation is the density of both occupied and unoccupied states:

$$P[E_{\text{incident}}, E_{\text{scattered}}] = \frac{2\rho(E_{\text{scattered}}) \int_{E_F}^{E_{\text{incident}} - E_{\text{scattered}}} \rho(E_e)\rho(E_h)dE_e}{\int_{E_F}^{E_{\text{incident}}} \int_{E_F}^{E_{\text{scattered}}} \rho(E_e)\rho(E_h)dE_e dE_{\text{scattered}}} ,$$

$$E_{\text{incident}} - E_{\text{scattered}} = E_e - E_h , \tag{3}$$

where $\rho(E)$ is the DOS at the energy E.[18]

Equation (3) is the probability that an electron scatters from E_{incident} to $E_{\text{scattered}}$ by the production of one electron-hole pair, but the same inelastic loss may also result from the creation of two or more electron-hole pairs. Assuming that each incident electron may create as many as two electron-hole pairs, the secondary-electron distribution $R(E_{\text{incident}}, E)$ inside a sample bombarded with electrons of energy E_{incident} is given by

$$R(E_{\text{incident}}, E) = \int_{E_F}^{E_{\text{incident}}} P[E_{\text{incident}}, E']P[E', E]dE' . \tag{4}$$

Similarly, Dose and co-workers[2,14,15] calculate $R(E_{\text{incident}}, E)$ for the case in which each incident electron could create up to n electron-hole pairs, by n repeated convolutions of Eq. (3). Unfortunately, there are many materials for which this method cannot be used due simply to the lack of a sufficiently accurate knowledge of the DOS over the necessary range in energy.

Turtle and Liedfeld[16] remove the inelastic background in x-ray BIS spectra of polycrystalline metals by using measured x-ray-photoemission (XPS) spectra to model $R(E_{\text{incident}}, E)$. The photoemission spectrum of a narrow core level and its inelastic tail approximates the inelastic spectrum of electrons produced by an incident monoenergetic electron beam in BIS if the kinetic energy of the photoemitted electron is equal to the kinetic energy of the incident electron beam. The measured line shapes of the core levels consisted of a flat background of height h superimposed on the low-kinetic-energy side of a sharp core level of area A. Turtle and Liedfeld[16] assumed that the ratio A/h is a constant for a given sample; in other words, the height of the background, h, depends only upon the number of photoexcited core-level electrons and the experimental parameters. $R(E_{\text{incident}}, E)$ is then approximated by the energy profile of the incident-electron beam plus a flat background located below the incident-beam energy. For a monoenergetic incident-electron beam (a δ function having area A), the electron energy distribution is given by

$$R(E_{\text{incident}}, E) = A\delta(E - E_{\text{incident}}) + h , \tag{5}$$

where $h = 0$ for $E > E_{\text{incident}}$. This is equivalent to the functional form of $R(E_{\text{incident}}, E)$ used in integral backgrounds,[6,7] with the added advantage that A/h is determined experimentally from an XPS spectrum instead of being a free parameter chosen by requiring the background in the measured BIS spectrum to pass through a chosen point.

The difficulty in using a core-level XPS spectrum to model $R(E_{\text{incident}}, E)$ in the energy range appropriate for *ultraviolet* IPES is that the final-state energy of the photoexcited electron should be of order 10 eV above the Fermi energy; in this energy range the XPS spectrum is dominated by secondary electrons. In some simple sense the number of low-energy secondary electrons produced by a single photoexcited electron is proportional to the energy above E_F of the photoexcited electron. Therefore, the inelastic background in the XPS spectrum is not dominated by the secondaries created by the photoexcited core-level electron—the signal we wish to measure—but by the secondaries created by higher-kinetic-energy electrons photoexcited from states having lower binding energies.

Woodruff *et al.*[1] allude to the use of EELS to approximate $R(E_{\text{incident}}, E)$ for use in ultraviolet IPES, but the only application of this method is to x-ray BIS spectra of polycrystalline metals.[17] [EELS spectra have been used previously by others to remove the inelastic background in XPS (Ref. 20) and AES (Refs. 21–23) spectra, but these applications involve somewhat different considerations than does IPES.]

B. Use of EELS spectra

$R(E_{\text{incident}}, E)$ may be approximated by a series of EELS spectra taken with primary-beam energies corresponding to each of the incident-beam energies used to measure the IPES spectrum. However, since the energy position and relative intensity of the features in our measured EELS spectra of polycrystalline Ag and single-crystal $V_2O_5(001)$ did not vary drastically upon changing the incident-beam energy, we approximate $R(E_{\text{incident}}, E)$ by a *single* EELS spectrum rigidly shifted such that the elastic peak is at the variable energy E_{incident}. [Previous BIS,[17] XPS,[20] and AES (Refs. 21–23) studies also used a single EELS spectrum.] The iterative deconvolution method of van Cittert[24] as described by Madden and Houston[21] was used to deconvolve Eq. (1).

IV. THE PRODUCTION OF BACKGROUND IN IPES

A description of inverse photoemission in a single crystal is shown in Fig. 2 using a schematic energy-band diagram. For our discussion of both angle-resolved and angle-integrated IPES we shall assume that a collimated electron beam is incident normal to the sample surface. In KRIPES the sample is a single crystal; thus the incident electron couples only to the initial states in the reduced Brillouin zone that lie along the line $k_{\parallel}=0$ (the Γ-K line in Fig. 2). In angle-integrated IPES from a polycrystalline sample, however, the incident electron may couple to states throughout the entire Brillouin zone.

Four processes can produce the photons measured in IPES: direct transitions (thick black arrow in KRIPES; thick black and striped arrows in angle-integrated IPES); indirect transitions (shaded arrow); inelastic scattering throughout the Brillouin zone (thin black arrows) followed by a direct (white arrows) or indirect radiative transition (not shown); and elastic scattering throughout the zone (thin dashed arrow) followed by a direct (striped arrow) or indirect radiative transition (not shown). In the following discussion we divide these four processes into two categories: true signal and background.

A. Angle-resolved IPES

Typically KRIPES is used to determine the energy and crystal momentum of unoccupied electron states. The conservation equations used to find the **k** value of a transition are derived from the three-step model of KRIPES (Refs. 1, 6, 10, and 25) in which the one-electron eigenfunctions are Bloch functions of an infinite lattice so that all optical transitions are direct, **k**-conserving transitions.[26] [The three-step model does not take into account indirect radiative transitions (shaded arrow).] Thus in KRIPES the direct optical transitions which occur without prior elastic or inelastic scattering comprise the true signal (black arrow), while the indirect transitions (shaded arrow) and radiative transitions preceded by either elastic (striped arrow) or inelastic scattering (white arrows) are background. We would like to remove the background (shaded, striped, and white arrows) using an EELS spectrum. However, since an EELS spectrum does not contain information about the **k** distribution of the scattered electrons, it is not possible to distinguish between transitions that occur at the same energy but at different points in the Brillouin zone (the black, shaded, and stripped arrows); therefore, the only background that one can hope to remove in a KRIPES spectrum is the background produced by inelastic scattering (white arrows).

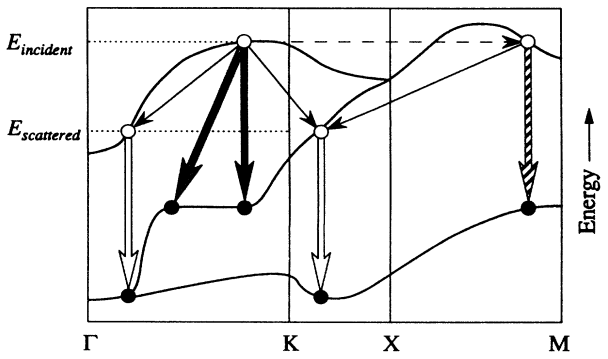

FIG. 2. A schematic energy-band diagram used to illustrate inverse photoemission processes. See text for details.

Equation (1) assumes that the probability that an electron *incident* at energy $E_{\text{scattered}}$ will emit an $\hbar\omega_0$ photon, $I_{\text{true}}(E_{\text{scattered}})$, is equal to the probability that an electron incident at energy E_{incident} which has already scattered to $E_{\text{scattered}}$ will emit an $\hbar\omega_0$ photon. However, electrons incident at $E_{\text{scattered}}$ couple only to states along Γ-K (primary electrons: left white arrow) while electrons that scatter from E_{incident} to $E_{\text{scattered}}$ are not restricted by conservation laws to states along Γ-K (scattered electrons: both white arrows). The differing distributions in **k** space of the primary and scattered electrons result in different probabilities of producing an $\hbar\omega_0$ photon; thus even if we knew the fraction of the incident beam that scatters from E_{incident} to $E_{\text{scattered}}$, $R(E_{\text{incident}},E_{\text{scattered}})dE$, we would not know how many of those scattered electrons emit $\hbar\omega_0$ photons from optical transitions along the Γ-K direction (left white arrow). As a result, the measured KRIPES spectrum at E_{incident} is not strictly the sum of the true signal at E_{incident} and the true signal at all lower energies weighted by the number of scattered electrons at each energy.

There are several physical processes which help to satisfy the approximations used in Eq. (1). Elastic scattering of some of the electrons incident at $E_{\text{scattered}}$ throughout the Brillouin zone (left→right white arrow) makes the primary and scattered electron **k** distributions more similar. Also, in an actual crystal the presence of the surface destroys the periodicity of the infinite lattice in the direction of the surface normal but does not affect the periodicity along any direction parallel to the surface;[27] the component of momentum parallel to the surface, $k_{\parallel}$, thus remains a good quantum number, but the allowed values of the perpendicular component $k_{\perp}$ are no longer discrete. As a result, optical transitions conserve $k_{\parallel}$ but not $k_{\perp}$, i.e., there are one-dimensional DOS effects in KRIPES (Refs. 1 and 10) (shaded arrow). The greater the extent to which the surface relaxes $k_{\perp}$ conservation in optical transitions, the less important are the differing **k** distributions of the primary and scattered electrons. Since **k** conservation is not completely relaxed, we must keep in mind that an isochromat is generated by an electron source inside the sample that is distributed in momentum as well as energy.

An electron incident at an energy $\hbar\omega_0$ above the Fermi energy that suffers an inelastic loss is not left with enough excess energy to produce an $\hbar\omega_0$ photon; thus there is no *inelastic* background at onset in KRIPES. However, an electron may scatter elastically prior to the radiative emission, and therefore an *elastic* background may be present even at the onset of emission in KRIPES. If the mean free path for elastic scattering is shorter than or comparable to the mean free path for inelastic scattering,[19] then many of the incident electrons will scatter elastically before scattering inelastically. In that case the

elastic background at threshold can be substantial. In two examples in the literature of background subtraction in KRIPES of single crystals (a hand-drawn[4,5] and a parabolic background[9]), one starts with zero background at threshold,[4] while the other uses a finite background at threshold.[9] If there are no direct transitions at threshold, then all of the measured signal at threshold is background produced by elastic scattering and/or indirect transitions.

B. Angle-integrated IPES

In **k**-integrated IPES, spectra are often compared directly with a calculated DOS,[9,28] making the emission produced by both elastic scattering (striped arrow) and indirect transitions (shaded arrow) a part of the signal we wish to measure. All momentum information about the measured transitions is lost since the incident beam sees many orientations of the crystal in **k**-integrated IPES, distributing the initial states of the incident electrons throughout the entire Brillouin zone. A feature in the true spectrum at energy E_{incident} is associated with any of the transitions throughout the zone that have an initial energy E_{incident} (the black, shaded, and striped arrows in Fig. 2); consequently there is no elastic background at or above threshold. The only background in **k**-integrated IPES is the inelastic background (white arrows)—precisely what Eq. (1) is best suited to model. We must, of course, still make the approximation that the primary and scattered electron distributions are the same—an approximation that is more nearly satisfied in angle-integrated IPES than in KRIPES.

V. RESULTS

Using Eq. (1) to model the production of background in IPES in conjunction with measured EELS spectra, we have determined inelastic backgrounds for both the KRIPES spectrum of V_2O_5(001) and the angle-integrated IPES spectrum of Ag.

A. KRIPES

Figure 3(a) shows a typical KRIPES spectrum of UHV-cleaved V_2O_5(001) taken in normal incidence (solid squares). Small changes in consecutively recorded KRIPES spectra of V_2O_5(001) were observed: the features broadened and lost intensity with each of the first few spectra recorded after a cleave. The changes in the spectra are presumably due to the production of defects by the incident-electron beam. Changes in the low-energy electron-diffraction pattern as a function of beam exposure time have been observed previously by others.[29] The measured EELS spectrum used to model $R(E_{\text{incident}},E)$ (solid line) yields a smooth inelastic background (open circles). The deconvolution result [Fig. 3(b)] approximates the KRIPES spectrum without inelastic background. The elastic background and the background resulting from all indirect radiative transitions having an initial-state energy equal to the incident-electron energy remain part of the deconvolution result.

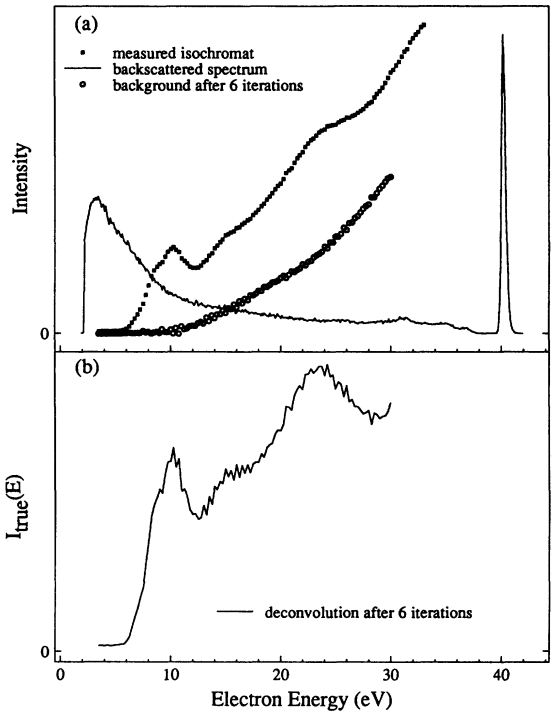

FIG. 3. (a) EELS spectrum of UHV-cleaved single-crystal V_2O_5(001) (solid line); measured normal-incidence IPES isochromat ($\hbar\omega_0=9.8$ eV) (squares); and the inelastic background (circles). (b) The corresponding true spectrum $I_{\text{true}}(E)$ after deconvolution using the measured EELS spectrum.

The secondary-electron distribution in all materials is characterized by a large feature at low kinetic energies that contains the majority of the inelastically scattered electrons [the feature at approximately 3 eV in Fig. 3(a)], but only those electrons that scatter to an energy greater than $\hbar\omega_0$ above E_F contribute to the background. In the EELS spectrum in Fig. 3(a), $\hbar\omega_0$ above E_F is located at a kinetic energy of $\hbar\omega_0+E_F-E_{\text{vac}}$ since the EELS spectrum is cut off by the vacuum level E_{vac} at zero kinetic energy. Thus electrons with a kinetic energy less than $\hbar\omega_0+E_F-E_{\text{vac}}$ will not contribute to the background since they do not have enough excess energy to produce an $\hbar\omega_0$ photon. If $\hbar\omega_0$ is large, the secondary-electron feature does not contribute to the inelastic background; however, for small isochromat energies these secondary electrons can have a large effect on the spectrum. Typically the low-energy secondary-electron peak produced by incident electrons in the energy range used in ultraviolet IPES extends to kinetic energies of less than 10 eV. Since a typical work function ($E_{\text{vac}}-E_F$) is around 5 eV, an isochromat energy less than about 15 eV has a large inelastic contribution from the secondary-electron feature.

B. Angle-integrated IPES

The measured EELS spectrum used to approximate $R(E_{\text{incident}},E)$ in polycrystalline Ag and the measured

isochromat are shown in Figs. 4(a) and 4(b), respectively. The deconvolution result is shown in Fig. 4(c) along with the calculated Ag DOS of Lässer, Smith, and Benbow.[30]

Since Eq. (1) is effectively a smoothing operation, features in both the true spectrum and the EELS spectrum are less pronounced in the measured spectrum. Compared to the large elastic peak, the rest of the EELS spectrum is relatively featureless, yielding a smooth background. It is possible that an EELS spectrum underestimates the intensity of the loss features in $R(E_{\text{incident}},E)$. For instance, those electrons that are elastically backscattered before passing through the surface region do not contribute to the measured IPES spectrum, but do contribute to the elastic peak in the EELS spectrum, thus underestimating the ratio of scattered to primary electrons. As the elastic peak height is reduced by numerical methods,[31] as is done in XPS (Ref. 32) and AES,[22] features will begin to appear in the background.[33] A portion of a modified EELS spectrum with an elastic peak height 0.6 times the measured amplitude is shown in Fig. 5(a). The inelastic backgrounds determined from the measured EELS spectrum and the modified EELS spectra with elastic peak heights of 0.6 and 0.3 times the measured elastic peak height are also shown in Fig. 5(a). A feature in the inelastic background emerges when the elastic peak amplitude is reduced to 0.3. Figure 5(b) shows the results of deconvoluting the isochromat using EELS spectra with elastic peak heights of 1.0, 0.6, and 0.3. We do not have a criterion for choosing the "best" elastic peak attenuation factor; i.e., the attenuation factor that produces a modified EELS spectrum which most closely resembles the actual inelastic spectrum of electrons inside the sample. However, using a reduced elastic-peak-height EELS spectrum to deconvolute the measured IPES spectrum may help to determine if any of the features present in the IPES spectrum are caused by inelastic losses.

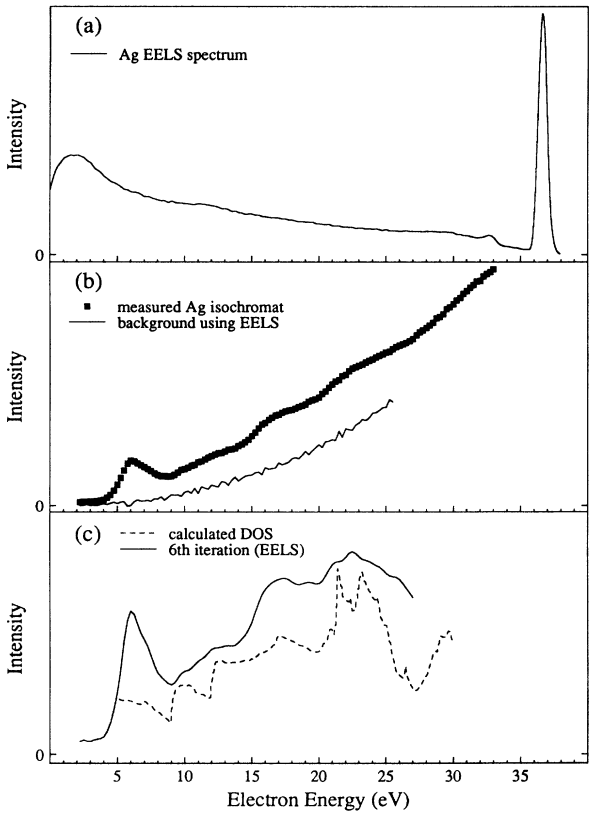

FIG. 4. (a) Measured EELS spectrum for polycrystalline Ag. (b) Measured IPES isochromat ($\hbar\omega_0=9.8$ eV) of polycrystalline Ag (squares), and the background determined by deconvoluting with the EELS spectrum in (a). (c) Comparison of the deconvolution result (solid line) with the Ag DOS calculation of Lässer, Smith, and Benbow (Ref. 30) (dashed line).

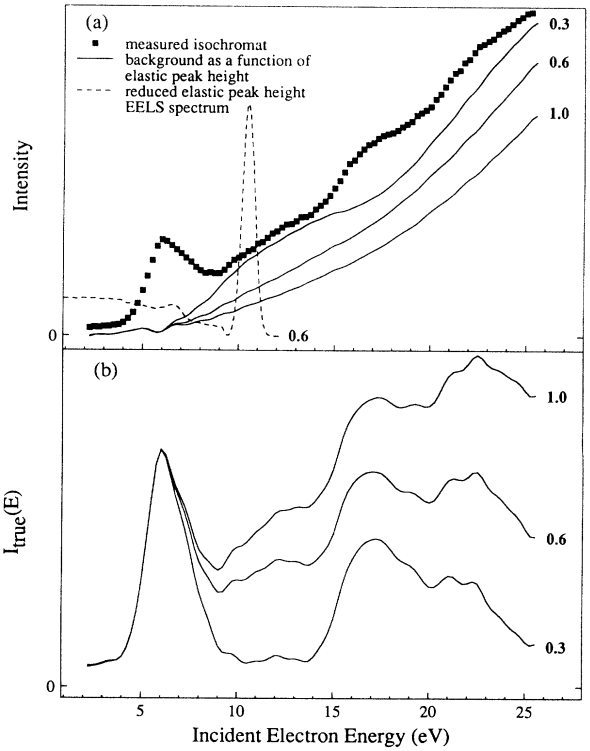

FIG. 5. (a) IPES isochromat spectrum ($\hbar\omega_0=9.8$ eV) of polycrystalline Ag (solid squares), an EELS spectrum in which the elastic peak height has been numerically reduced to 60% (dashed line), and inelastic backgrounds determined from EELS spectra with elastic peak amplitudes of 0.3, 0.6, and 1.0 times the measured elastic peak height (solid lines). (b) The deconvolution results $I_{\text{true}}(E)$ using fractional elastic peak heights of 0.3, 0.6, and 1.0.

VI. CONCLUSIONS

The differences in intent and experimental geometry between angle-resolved and angle-integrated IPES lead to two separate definitions of what constitutes the true signal and what is background in each of these two modes of inverse photoemission. The current model of background production used in the literature only accounts for one type of background—inelastic background, which is also the total background in angle-integrated IPES, but only a portion of the background in angle-

resolved IPES. In order to perform the background subtraction, one must determine the spectrum of inelastically scattered electrons inside the sample. In this paper we have discussed the approximations used in models of background production and have determined the inelastic spectrum by using experimentally measured electron-energy-loss spectra. Examples of inelastic background subtraction using the experimentally determined inelastic spectrum are presented for both angle-resolved and angle-integrated IPES spectra.

ACKNOWLEDGMENT

This work was partially supported by NSF Solid State Chemistry Grant No. DMR90-15488.

[1]D. P. Woodruff, N. V. Smith, P. D. Johnson, and W. A. Royer, Phys. Rev. B **26**, 2943 (1982).
[2]V. Dose, Prog. Surf. Sci. **13**, 225 (1983).
[3]N. V. Smith, Rep. Prog. Phys. **51**, 1227 (1988); F. J. Himpsel, Surf. Sci. Rep. **12**, 1 (1990).
[4]R. Baptist, A. Pellissier, and G. Chauvet, Solid State Commun. **68**, 555 (1988).
[5]P. A. Bruhwiler, G. M. Watson, E. W. Plummer, H.-J. Sagner, and K.-H. Frank, Europhys. Lett. **11**, 573 (1990).
[6]P. O. Nilsson and C. G. Larrson, Jpn. J. Appl. Phys. **17**, 144 (1978).
[7]P. O. Nilsson and A. Kovacs, Phys. Scr. T **4**, 61 (1983); E. Puppin, L. Braincovich, B. DeMichelis, P. Vavassori, and E. Vescovo, Surf. Sci. **264**, 429 (1992).
[8]E. Bertel, N. Memmel, W. Jacob, V. Dose, F. P. Netzer, G. Rosina, G. Rangelov, G. Astl, N. Rösch, P. Knappe, B. I. Dunlap, and H. Saalfeld, Phys. Rev. B **39**, 6087 (1989).
[9]A. K. See, M. Thayer, and R. A. Bartynski, Phys. Rev. B **47**, 13 722 (1993).
[10]V. Dose and Th. Fauster, Solid State Commun. **50**, 67 (1984).
[11]The electron gun used is based on the design by N. G. Stoffel and P. D. Johnson, Nucl. Instrum. Methods A **234**, 230 (1985).
[12]The photon detector used is based on the design described in the following papers: N. Babbe, W. Drube, I. Schäfer, and M. Skibowski, J. Phys. E **18**, 158 (1985); I. Schäfer, W. Drube, M. Schlüter, G. Plagemann, and M. Skiboski, Rev. Sci. Instrum. **58**, 710 (1986).
[13]Perkin-Elmer, PHI Model 15-255G Precision Electron Energy Analyzer.
[14]V. Dose, J. Phys. Chem. **88**, 1681 (1984).
[15]V. Dose, Th. Fauster, and H. Scheidt, J. Phys. F **11**, 1801 (1981); H. Scheidt, Fortschr. Phys. **31**, 357 (1983).
[16]R. R. Turtle and R. J. Liedfeld, Phys. Rev. B **7**, 3411 (1973).
[17]D.v.d. Marel, G. A. Sawatzky, R. Zeller, F. U. Hillebrecht, and J. C. Fuggle, Solid State Commun. **50**, 47 (1984); W. Speier, R. Zeller, and J. C. Fuggle, Phys. Rev. B **32**, 3597 (1985).
[18]E. O. Kane, Phys. Rev. **159**, 624 (1967).
[19]C. N. Berglund and W. E. Spicer, Phys. Rev. **136**, A 1030 (1964).
[20]M. F. Koenig and J. T. Grant, J. Electron Spectrosc. Relat. Phenom. **33**, 9 (1984).
[21]H. H. Madden and J. E. Houston, J. Appl. Phys. **47**, 3071 (1976).
[22]H. H. Madden and J. E. Houston, J. Vac. Sci. Technol. **14**, 412 (1977).
[23]W. M. Mularie and W. T. Peria, Surf. Sci. **26**, 125 (1971).
[24]P. H. van Cittert, Z. Phys. **69**, 298 (1931); H. C. Burger and P. H. van Cittert, *ibid.* **79**, 722 (1932); **81**, 428 (1933).
[25]For an analogous discussion in the context of photoemission, see M. Cardona and L. Ley, in *Photoemission in Solids I,* edited by M. Cardona and L. Ley (Springer-Verlag, Berlin, 1978), p. 1.
[26]Radiative transitions are direct transitions in the three-step model if we ignore the photon momentum and use the dipole approximation.
[27]Even if the surface reconstructs, $k_{\|}$ is a good quantum number as long as the reconstruction is periodic.
[28]V. Dose and G. Reusing, Appl. Phys. **23**, 131 (1980). BIS is better suited for measuring the DOS than ultraviolet IPES.
[29]L. Fiermans and J. Vennik, Surf. Sci. **9**, 187 (1968).
[30]R. Lässer, N. V. Smith, and R. L. Benbow, Phys. Rev. B **244**, 1895 (1981).
[31]A Gaussian was fitted to and then subtracted from the measured EELS spectrum, leaving an EELS spectrum without an elastic peak. The modified EELS spectra were then produced by multiplying the Gaussian by 0.3 or 0.6 and then adding the result to the EELS spectrum without an elastic peak.
[32]D. A. Shirley, Phys. Rev. B **5**, 4709 (1971).
[33]A discussion of the appropriateness of using an EELS spectrum to remove background in Auger and XPS is given by J. A. D. Matthew and P. R. Underhill, J. Electron Spectrosc. Relat. Phenom. **14**, 371 (1978).

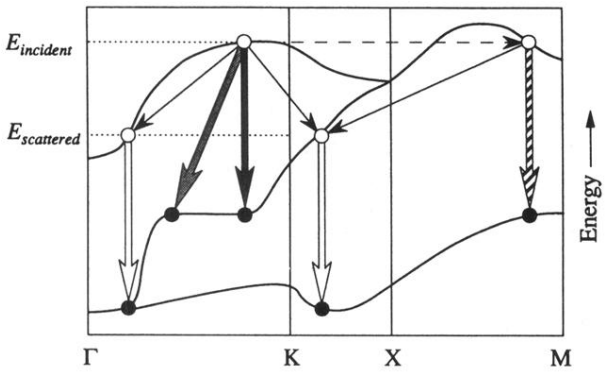

FIG. 2. A schematic energy-band diagram used to illustrate inverse photoemission processes. See text for details.